
Article:

Tahir, B.A. orcid.org/0000-0003-0531-3519, Marshall, H., Hughes, P.J.C. et al. (4 more authors) (2019) Comparison of CT ventilation imaging and hyperpolarised gas MRI: effects of breathing manoeuvre. Physics in Medicine and Biology, 64 (5). 055013. ISSN 0031-9155

https://doi.org/10.1088/1361-6560/ab0145

Physics in Medicine and Biology

ACCEPTED MANUSCRIPT

Comparison of CT ventilation imaging and hyperpolarised gas MRI: effects of breathing manoeuvre

To cite this article before publication: Bilal A Tahir *et al* 2019 *Phys. Med. Biol.* in press https://doi.org/10.1088/1361-6560/ab0145

Comparison of CT ventilation imaging and hyperpolarised gas MRI: Effects of breathing manoeuvre

Bilal A Tahir[1,2], Helen Marshall[1], Paul JC Hughes[1], Christopher E Brightling[3], Guilhem Collier[1], Rob H Ireland[1,2], Jim M Wild[1]

[1]POLARIS, Academic Radiology, University of Sheffield, UK

[2]Academic Unit of Clinical Oncology, University of Sheffield, UK

[3]Institute for Lung Health, University of Leicester, UK

Abstract

Image registration of lung CT images acquired at different inflation levels has been proposed as a surrogate method to map lung 'ventilation'. Prior to clinical use, it is important to understand how this technique compares with direct ventilation imaging modalities such as hyperpolarised gas MRI. However, variations in lung inflation level have been shown to affect regional ventilation distributions. Therefore, the aim of this study was to evaluate the impact of lung inflation levels when comparing CT ventilation imaging to ventilation from ^{3}He-MRI.

7 asthma patients underwent breath-hold CT at total lung capacity (TLC) and functional residual capacity (FRC). ^{3}He-MRI and a same-breath ^{1}H-MRI were acquired at FRC+1L and TLC. Percentage ventilated volumes (%VVs) were calculated for FRC+1L and TLC ^{3}He-MRI. TLC-CT and registered FRC-CT were used to compute a surrogate ventilation map from voxel-wise intensity differences in Hounsfield unit values, which was thresholded at the 10th and 20th percentiles. For direct comparison of CT and ^{3}He-MRI ventilation, FRC+1L and TLC ^{3}He-MRI were registered to TLC-CT indirectly via the corresponding same-breath ^{1}H-MRI data. For ^{3}He-MRI and CT ventilation comparison, Dice similarity coefficients (DSCs) between the binary segmentations were computed.

The median (range) of %VVs for FRC+1L and TLC ^{3}He-MRI were 90.5 (54.9-93.6) and 91.8 (67.8-96.2), respectively (p=0.018). For MRI versus CT ventilation comparison, statistically significant improvements in DSCs were observed for TLC ^{3}He MRI when compared with FRC+1L, with median (range) values of 0.93 (0.86-0.93) and 0.86 (0.68-0.92), respectively (p=0.017), for the 10-100th percentile and 0.87 (0.83-0.88) and 0.81 (0.66-0.87), respectively (p=0.027), for the 20-100th percentile.

Correlation of CT ventilation imaging and hyperpolarised gas MRI is sensitive to lung inflation level. For ventilation maps derived from CT acquired at FRC and TLC, a higher correlation with gas ventilation MRI can be achieved if the MRI is acquired at TLC.

Keywords: CT ventilation imaging, functional lung imaging, hyperpolarised gas MRI, lung inflation, lung diseases, pulmonary image registration

Novelty & Significance

CT ventilation imaging derived from lung CT images acquired at different inflation levels has been proposed as a surrogate method to map lung ventilation. However, it is important to understand how the technique compares with established ventilation modalities such as hyperpolarised gas MRI. Direct comparison of CT ventilation imaging and gas ventilation MRI requires consideration of the sensitivity of both modalities to lung inflation state. To date, CT ventilation has not been compared against an established ventilation imaging modality acquired at different inflation states. Here, we report the first study to evaluate the impact of lung inflation level when comparing gas MRI and CT ventilation.

1. Introduction

The primary function of the human lungs is gas exchange of which ventilation is an essential component. Although normal lungs exhibit a degree of ventilation heterogeneity (Crawford *et al.*, 1985), a marked increase has been shown in patients with respiratory diseases (Mugler *et al.*, 2010). In current clinical practice, ventilation is normally evaluated using global measures of lung function. Assessment of the regional heterogeneity of respiratory disease, however, requires imaging techniques, which are able to visualise and quantify the spatially varying extent of ventilation.

Several respiratory diseases are characterised by impaired lung function on a regional basis with anatomically specific propensity of lung obstruction. In particular, obstructive lung diseases such as asthma, chronic obstructive pulmonary disease (COPD) and cystic fibrosis (CF) exhibit marked increases in ventilation heterogeneity when compared with normal subjects due to airway narrowing or closure. For asthmatics, the impact of regionally specific therapeutic interventions such as bronchial thermoplasty may benefit from the regional and quantitative information yielded by ventilation imaging from treatment planning to the assessment of regional pathophysiology response to treatment (Thomen *et al.*, 2015). For COPD patients, regional ventilation can help assess the impact of lung volume reduction surgery (Kurose *et al.*, 2004). For paediatric patients with cystic fibrosis, an early detection of ventilation dysfunction may enable bronchoscopy or physiotherapy for regionally specific mucus clearance to prevent the onset of lung disease irreversibility (Thomen *et al.*, 2015). Regional lung ventilation imaging techniques including single photon emission computed tomography (SPECT) (Seppenwoolde *et al.*, 2000; Christian *et al.*, 2005) and hyperpolarised gas magnetic resonance imaging (Ireland *et al.*, 2007) have also been applied to lung cancer patients undergoing radiotherapy to spatially assist in preferential sparing of functional lung during the treatment planning process (Ireland *et al.*, 2016). Thus, the ability to visualise and quantify regional lung ventilation is highly desirable. However, current regional ventilation modalities suffer from some

or all of the following: poor spatial and temporal resolution, requirement of inhaled contrast agents and specialised equipment inaccessible to most centres.

Computed tomography (CT) images of the lungs are routinely utilised in the clinic for the radiological assessment of respiratory diseases and radiotherapy treatment planning. Over the past decade, CT-based methods of mapping regional ventilation, sometimes referred to as 'CT ventilation imaging', which are based on image registration of non-contrast lung CT images acquired at two different inflation levels, have been proposed as a surrogate method to image lung 'ventilation' (Guerrero *et al.*, 2005; Reinhardt *et al.*, 2008). Although the technique has gained considerable interest, relatively few papers have addressed the issue of validation against established direct ventilation imaging modalities such as hyperpolarised gas MRI (Mathew *et al.*, 2012; Tahir *et al.*, 2016; Tahir *et al.*, 2018). However, direct comparison of CT ventilation imaging and gas ventilation MRI requires consideration of the potential sensitivity of both methods to lung inflation state. For example, hyperpolarised gas ventilation MRI has been shown to be sensitive to lung inflation state; in elite divers, marked decreases in ventilation were demonstrated at sub-residual volumes (Muradyan *et al.*, 2010), and in patients with asthma, increased and more homogeneous ventilation was visualised in images acquired at total lung capacity (TLC) when compared to those acquired at functional residual capacity (FRC) + 1L (Marshall *et al.*, 2013).

Similarly, CT-based surrogates of ventilation have been shown to be sensitive to inflation state; previously, Mistry *et al.* (2013) evaluated the effects of different breathing manoeuvres during CT imaging and observed marked differences in the distribution of the computed CT ventilation images. To date, CT-based surrogates of ventilation have not been compared against an established direct ventilation imaging modality acquired at different inflation states.

The primary aim of this study, therefore, was to evaluate the impact of inflation levels when CT-based surrogate maps of ventilation are compared against an established direct measure of regional ventilation. To this end, we employed ^{3}He hyperpolarised gas MR ventilation imaging acquired at breath-hold at two different lung volumes and performed spatial overlap comparison between each inflation state and the CT ventilation surrogate. A secondary aim was to evaluate the differences in ^{3}He ventilation with lung inflation state.

2. Methods

2.1. Subjects

The study was performed with national research ethics committee approval. Between September 2012 to February 2013, seven patients with sputum eosinophilia and moderate-to-severe asthma gave written informed consent to participate in this study. The inclusion criteria were greater than 18 years of age, physician diagnosis of asthma, currently on Global Initiative for Asthma (GINA) step 2 to 5 asthma therapies, sputum eosinophil count greater than or equal to 2%. The exclusion criteria included other acute illnesses, recent or current lower respiratory tract infection, contra-indication to MRI, body mass index <17 or >40 kg/m^2, women of child-bearing potential and patients who have been hospitalized or required high-dose (>10mg prednisolone/day) oral corticosteroid (OCS) therapy within 6 weeks of the screening visit. The characteristics of these patients can be found in Table 1.

Table 1 Summary of patient characteristics and lung function parameters.

	Age	Sex	FEV_1 (L)	FEV_1 (% predicted)	FEV_1/FVC (%)
1	41	Male	3.35	89.10	68.65
2	51	Female	0.80	33.81	45.71
3	45	Male	3.85	104.42	67.54
4	64	Female	2.10	107.03	72.41
5	62	Male	2.30	69.21	50.00
6	52	Female	2.10	99.81	74.73
7	42	Male	3.30	99.97	77.65
Mean	51	N/A	2.54	86.19	65.24
SD	9.20	N/A	1.03	26.40	12.42

FEV_1 = forced expiratory volume in the first second of expiration, FVC = forced vital capacity, L = litres.

2.1. Image acquisition

All patients underwent CT and MRI. MRI was performed within 4 days of CT with a mean±SD interval of 1.5±0.8 days and range of 1 to 4 days.

Breath-hold CT scans were acquired at TLC and FRC on a Sensation 16 scanner (Siemens, Forchheim, Germany). The following CT settings were used: tube voltage, 120kV; tube current,

120mAs; rotation time, 0.5s; pitch, 1.5. Where available, a B30f reconstruction kernel was used or the next kernel closest to it (e.g. B35f, B60 etc.). CT in-plane resolution was approximately 0.86×0.86mm with a pixel matrix of 512×512. CT slice thickness was 1 mm with approximately 600 slices for each patient.

^{3}He MR ventilation images were acquired at two lung inflation states, namely, FRC+1L and TLC, during separate breath-holds in a manner similar to Smith *et al.* (2018) described briefly as follows. In the same breath-hold as ^{3}He MRI, anatomical ^{1}H MR images were also acquired on a GE HDx 1.5T whole body MRI system (GE Healthcare, Milwaukee, WI, USA) (Wild *et al.*, 2011). For the ^{3}He MR ventilation images acquired at FRC+1L, patients exhaled to FRC and then inhaled a mixture of 350ml ^{3}He and 650ml N_2. For the ^{3}He MR ventilation images acquired at TLC, patients exhaled to FRC and then inhaled a mixture of 400ml ^{3}He and 600ml N_2 followed by inhalation of room air until TLC was reached. The increase in ^{3}He dose was to account for the gas dilution with increase in lung volume at TLC. Ventilation images at TLC were acquired within six minutes of those at FRC+1L.

Helium was polarised on-site to approximately 25% using a rubidium spin exchange polariser (GE Healthcare, Amersham, UK). A transmit-receive quadrature ^{3}He vest coil (Clinical MR Solutions, Brookfield, WI, USA) was used to acquire ^{3}He images with the following sequence: 2D spoiled gradient-echo, 3x3mm in-plane resolution, 10mm slice thickness, 38.4cm field of view, 1.1ms echo time, 3.6ms repetition time, 8° flip angle, 62.5kHz bandwidth and full lung coverage (20 to 24 slices). Same-breath ^{1}H images from the same coronal slices were acquired using the ^{1}H body coil of the scanner with the following sequence; 2D steady state free precession, 3x6mm in-plane resolution, 38.4cm field of view, 0.7ms echo time, 2.4ms repetition time, 50° flip angle, and 167kHz bandwidth. The MRI acquisition protocol was described in Smith *et al.* (2018) and Hughes *et al.* (2018).

2.3. Image segmentation

Medical image segmentation software (Mimics; Materialise, Leuven, Belgium) was used to segment the lungs of the inspiratory and expiratory CT scans. ^{3}He and ^{1}H MR lung parenchyma were segmented in Matlab (MathWorks, Natick, MA) using a modified version of the Spatial Fuzzy C-means (FCM) algorithm presented by Chuang *et al.* (2006) as recently described (Hughes *et al.*, 2017). Prior to segmentation, images were pre-processed using a bilateral filter (Tomasi and Manduchi, 1998). Segmented images were manually inspected and large airways including the trachea were removed.

2.4. Inspiratory and expiratory breath-hold CT image registration validation and algorithmic optimisation

CT ventilation imaging is highly sensitive to the image registration technique (Yamamoto *et al.*, 2011; Latifi *et al.*, 2013). In order to generate robust maps, accurate registration of inspiratory and expiratory CT images is essential. The vast majority of CT ventilation validation studies to date have utilised 4D-CT data, acquired during tidal breathing (Mathew *et al.*, 2012; Castillo *et al.*, 2012; Castillo *et al.*, 2010). However, the spatial displacement magnitudes between the maximum inhale and exhale phases of normal tidal breathing are significantly lower than those of paired breath-hold CT images acquired at the extremes of inflation (Castillo *et al.*, 2013). As such, inspiratory and expiratory breath-hold CT pose significant challenges for deformable image registration. Although several pulmonary CT datasets for validation of deformable registration exist (Vandemeulebroucke *et al.*, 2011), given the large differences between inspiratory and expiratory breath-hold CT used in this study, image registration was validated by computing the mean target registration error (TRE) of 300 corresponding expert landmarks on inspiratory and expiratory breath-hold image pairs from a separate validation cohort consisting of CT images from ten COPD patients. The paired images were acquired at the same inflation levels as the breath-hold CT scans used for this study (TLC and FRC). These data sets were obtained from the DIR-lab (www.dir-lab.com), a publicly available reference dataset acquired from the National Heart Lung Blood Institute COPDgene study archive for the validation of pulmonary deformable registration algorithms (Castillo *et al.*, 2013). The in-plane resolution of the images ranged from 0.586x0.586 to 0.742x0.742 mm. Slice thickness was always 2.5 mm. The TRE was computed by taking the Euclidean distance between the corresponding landmark on the fixed and warped moving image.

In this study, the choice of registration software used was based on the best performing algorithm at the time of writing during a recent pulmonary image registration competition (EMPIRE10, http://empire10.isi.uu.nl/), which forms part of the MICCAI Grand Challenges in image analysis. The results of this challenge were reported in Murphy *et al.* (2011) where the Greedy symmetric normalization (SyN) algorithm implemented within the Advanced Normalization Tools (ANTs) registration framework (Avants *et al.*, 2011) attained first place.

To find the optimal parameters for this dataset, a number of parameters were varied, and the mean TRE per patient was calculated. Initial parameters used were based on the developers' own submissions to the EMPIRE10 challenge (http://empire10.isi.uu.nl/mainResults.php) where two variants of their Symmetric Normalization (SyN) algorithm were used, one with Gaussian regularization and the other with B-splines. These two settings are referred to here as 'EMPIRE10_Syn' and 'EMPIRE10_BSplineSyn', respectively. Numerous experiments were undertaken to find the optimal parameters for the reference datasets with respect to minimising TRE.

In this study, we compare the results of these two scripts with that of an empirically validated optimised parameter script, referred to here as 'Optimised'.

All three methods are discussed in brief below:

1. EMPIRE10_Syn

- A coarse pre-alignment rigid transform was applied to align the centres of mass of the fixed and moving image intensities.
- The resulting transform was then applied to rigid and affine stages using the mutual information similarity metric with 32 histogram bins optimised via the gradient descent algorithm with a step size of 0.1.
- A multi-resolution Gaussian pyramid with 4 levels was used with down-sampling factors 8x4x2x1 and corresponding smoothing Gaussian sigmas of 3x2x1x0 mm.
- A maximum of 10,000 iterations was set for each resolution level to ensure convergence (Glocker *et al.*, 2011).
- For the non-rigid stage, the SyN diffeomorphic transform was used with a Gaussian regularization kernel width of 3 voxels for smoothing of the update transform field.
- A 4-level multi-resolution pyramid with down-sampling factors of 6x4x2x1 and corresponding smoothing Gaussian sigmas of 3x2x1x0 mm and the normalized correlation coefficient similarity metric with a radius of 4 voxels were used.
- A step size of 0.1 was selected for the gradient descent optimisation algorithm.

2. EMPIRE10_BSplineSyn

- For the rigid and affine stages, the same parameters as above were employed.
- An additional diffeomorphic transformation with explicit B-spline regularization (Tustison and Avants, 2013) that copes with larger deformations than the familiar SyN algorithm (Avants *et al.*, 2008) was applied instead to the resulting transform of the affine pipeline with a knot spacing for the update field of 40 mm.
- The same 4-level multi-resolution strategy was employed.

3. Optimised

- The empirically optimised script used identical rigid and affine parameters as EMPIRE10_Syn and EMPIRE10_BSplineSyn.
- For the deformable stage, the explicit B-spline regularization was applied to the resulting transform of the affine pipeline.

- A knot spacing for the update field of 65 mm provided optimal results.
- Additionally, a 5-level multi-resolution pyramid was used (instead of 4 levels) with down-sampling factors of 10x6x4x2x1 and corresponding smoothing Gaussian sigmas of 5x3x2x1x0 mm and the normalized correlation coefficient similarity metric with a radius of 2 voxels instead of 4.
- A step size of 0.2 was selected for the gradient descent optimisation algorithm.

To reduce the computational times in performing the three registration pipelines above, 8 cores via an Intel Xeon E5-2670 eight-core processor @ 2.60 GHz were run in parallel on a 64-bit high performance Linux server (Iceberg, University of Sheffield) using the multi-threading options available in ITK[4].

2.5. CT ventilation computation

For the CT ventilation calculation, FRC-CT was registered to TLC-CT using the optimised script. Next, TLC-CT and registered FRC-CT were used to compute a surrogate ventilation image from voxel-wise intensity differences in Hounsfield unit (HU) values based on a modified version of the original formulation of Guerrero *et al.* (2005) to account for the computation being performed in the inhalation CT spatial domain:

$$\frac{\Delta V}{V_{exp}} = 1000\frac{HU_{ins} - \overline{HU}_{exp}}{\overline{HU}_{exp}(1000 + HU_{ins})}$$

where $\overline{HU}_{exp}$ is the HU of the voxels in the moving deformed expiration image which spatially correspond to the voxels in the fixed inspiration image and HU_{insp} is the HU of the inspiratory voxel. The metric purports to be a measure of change in fractional content of air per voxel between respiratory phases.

For subsequent analysis, the CT ventilation surrogate image needed to be segmented. Here, we employed the percentile threshold technique used in several studies (Castillo *et al.*, 2010; Castillo *et al.*, 2012; Kipritidis *et al.*, 2014; Yamamoto *et al.*, 2014) to discern ventilated from non-ventilated lung. To assess the effect of using different percentile values, we thresholded the CT ventilation surrogate to the 10-100th and 20-100th percentile ranges which were assumed to be ventilated.

2.6. Comparison of ^{3}He MRI and CT

The percentage ventilated volume (%VV) was calculated for each patient by taking the ratio of the binary lung segmentations of ^{3}He and ^{1}H MRI. For spatial comparison of ^{3}He MRI and CT ventilation, for each patient, MR images were registered to the TLC-CT image's spatial domain via the anatomical same-breath ^{1}H MRI as previously described (Tahir *et al.*, 2014) and Dice similarity coefficients (DSCs) were computed separately for the binary segmentations of both CT ventilation percentiles with that of FRC+1L and TLC ^{3}He MRI. The workflow for the comparison method of FRC+1L and TLC ^{3}He MRI with CT ventilation is shown in Figure 1.

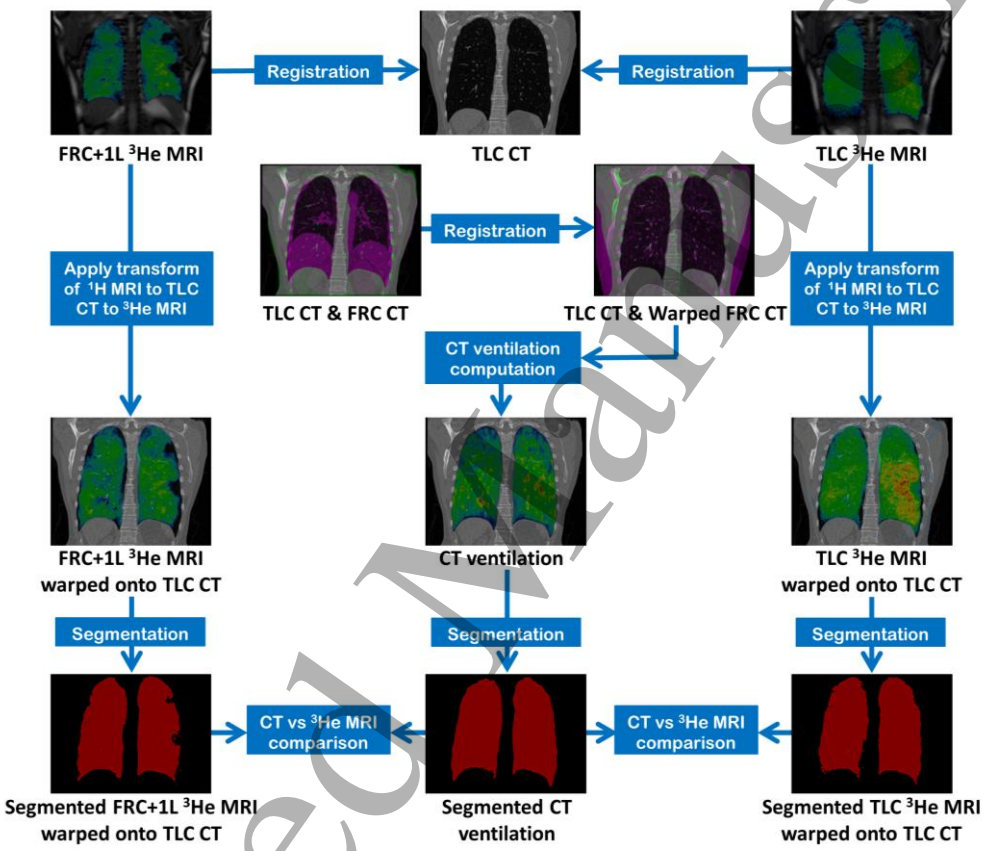

Figure 1 Workflow for comparison of FRC+1L and TLC ^{3}He MRI with CT ventilation. CT ventilation images were generated on TLC-CT geometry by deformably registering FRC-CT to TLC-CT. For each patient, ^{3}He MR images were registered to the TLC-CT image's spatial domain via the anatomical same-breath ^{1}H MRI. For spatial comparison, Dice similarity coefficients were computed separately for the binary segmentations of the CT ventilation images with that of the warped FRC+1L and TLC ^{3}He MR images.

2.7. Statistical analysis

Statistical analysis was performed by using IBM SPSS software (version 20.0; Chicago, Il, USA). A p value less than 0.05 was considered statistically significant. The Wilcoxon signed-ranks test was used to test statistical significance in differences.

3. Results

3.1. Breath-hold CT image registration accuracy

Figure 2 shows example coronal slices for the moving exhalation image overlaid with the fixed inhalation image for patient 10 of the DIR lab dataset before and after performing each of the three registration pipelines. There is a notable improvement in diffeomorphic registration accuracy with B-spline regularisation for both the EMPIRE10_BSplineSyn and Optimised pipelines and subtle improvements for the Optimised pipeline. The mean TREs before registration and for the registration pipelines are displayed in Table 2. The results show that B-spline regularisation improves registration accuracy compared with that of Gaussian regularisation ($p < 0.05$). The optimised script proposed in this study outperformed all other methods ($p < 0.05$).

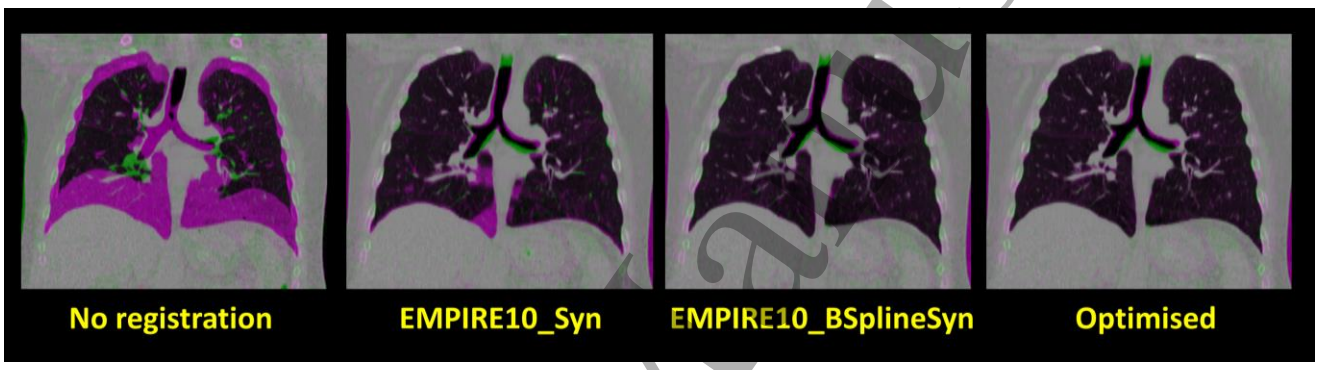

Figure 2 Example coronal slices for the moving exhalation image overlaid with the fixed inhalation image for patient 10 of the DIR lab dataset before and after performing each of the three registration pipelines.

Table 2 Registration accuracy results. Mean and standard deviation of the TREs of the 300 expert landmarks for breath-hold CT reference dataset. Values are given in mm. Summary statistics are shown for the registration methods compared in this study. Euclidian distances between landmarks when no registration was performed are provided for reference.

Registration method	Mean TRE±SD (mm)
0. No registration	23.36±10.11
1. EMPIRE10_Syn	7.98±3.49
2. EMPIRE10_BSplineSyn	3.09±1.53
3. Optimised	1.26±0.27

3.1. FRC+1L versus TLC ^{3}He MRI

All patients complied with the imaging procedures and were able to perform breath-holds at both FRC+1L and TLC. TLC ^{3}He MRI exhibited increased and more homogenous ventilation than FRC+1L ^{3}He MRI. Frequently, defects observed at FRC+1L would either partially or completely resolve at TLC. The spatial extent and location of these ventilation defects were confirmed by same-breath anatomical ^{1}H MRI as shown in Figure 3, indicating increased airway opening at the higher inflation state. The median (range) of %VV for FRC+1L and TLC ^{3}He MRI were 90.5 (54.9-93.6) and 91.8 (67.8-96.2), respectively (p=0.018). This is also displayed graphically in Figure 4.

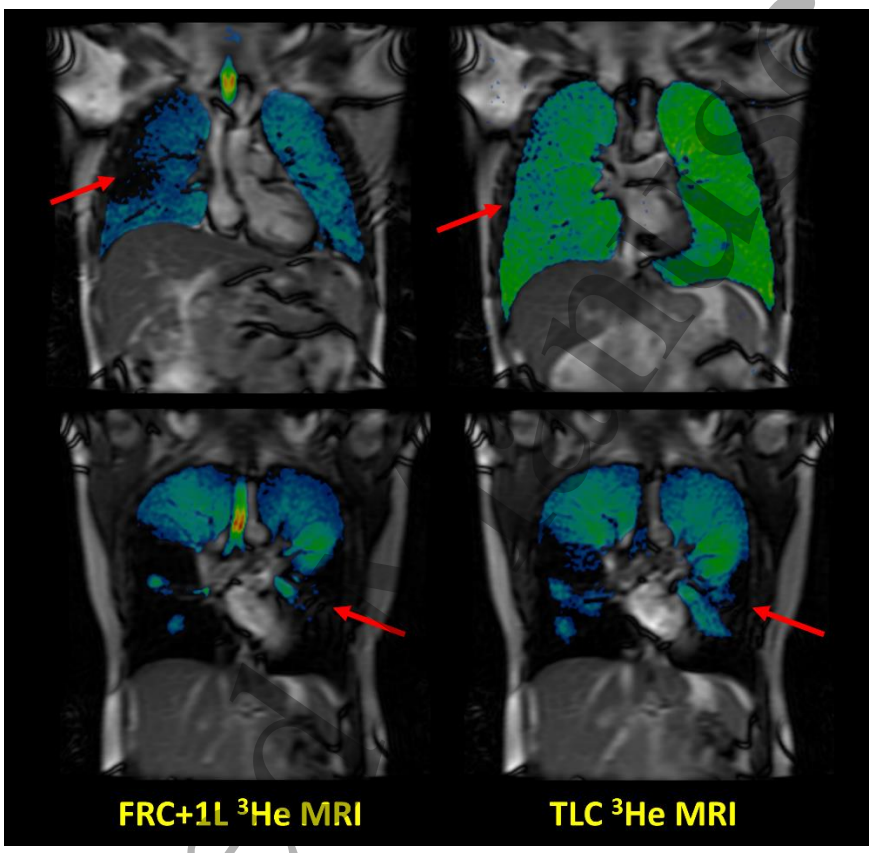

Figure 3 Corresponding coronal slices of patient 1 (top) and 2 (bottom) showing ^{3}He MRI acquired at FRC+1L (left) and TLC (right) fused with same-breath anatomical ^{1}H MRI. Some ventilation defects observed at FRC+1L resolve at TLC (red arrows), indicating increased

airway opening at the higher inflation state.

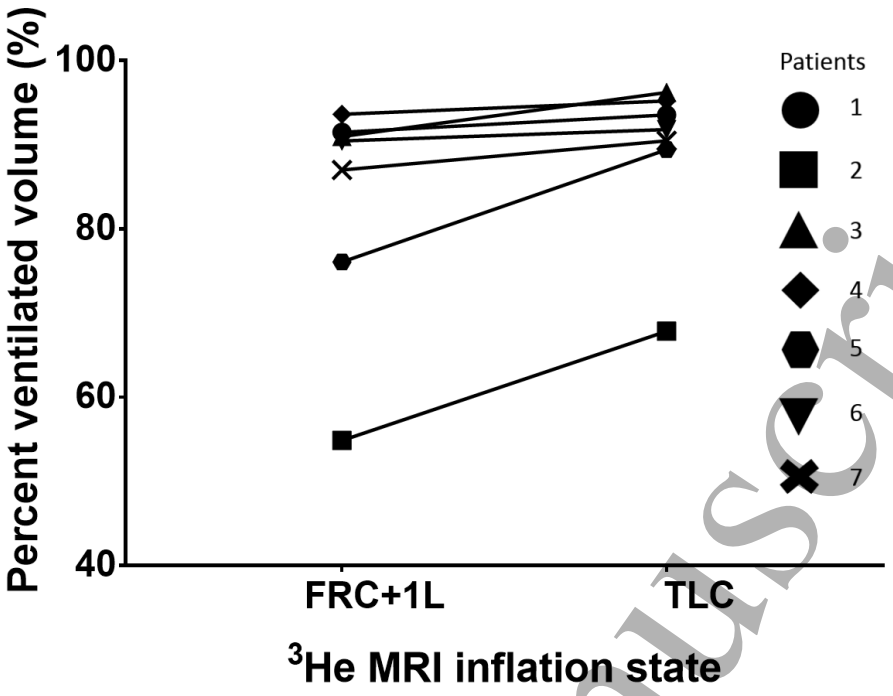

Figure 4 A comparison of percent ventilated volumes of ^{3}He MRI acquired at FRC+1L and TLC. Individual data points are shown for all patients.

3.2. CT ventilation vs FRC+1L and TLC ^{3}He MRI

Figure 5 shows corresponding coronal slices of registered FRC+1L and TLC ^{3}He MRI and CT ventilation for two patients in the study. The CT ventilation images are visually more similar to those of the TLC ^{3}He MRI. This was confirmed by quantitative spatial overlap results, whereby statistically significant improvements in DSCs were observed between CT ventilation and TLC ^{3}He MRI compared with FRC+1L ^{3}He MRI, with median (range) values of 0.93 (0.86-0.93) and 0.86 (0.68-0.92) respectively, for the 10-100th percentile (p=0.017) and 0.87 (0.83-0.88) and 0.81 (0.66-0.87) respectively, for the 20-100th percentile (p=0.027). Statistically significant improvements in DSCs were observed with the 10-100th compared with the 20-100th percentile CT ventilation masks for both FRC+1L (p = 0.026) and TLC ^{3}He MRI (p = 0.017). The results for each patient are displayed in Table 3.

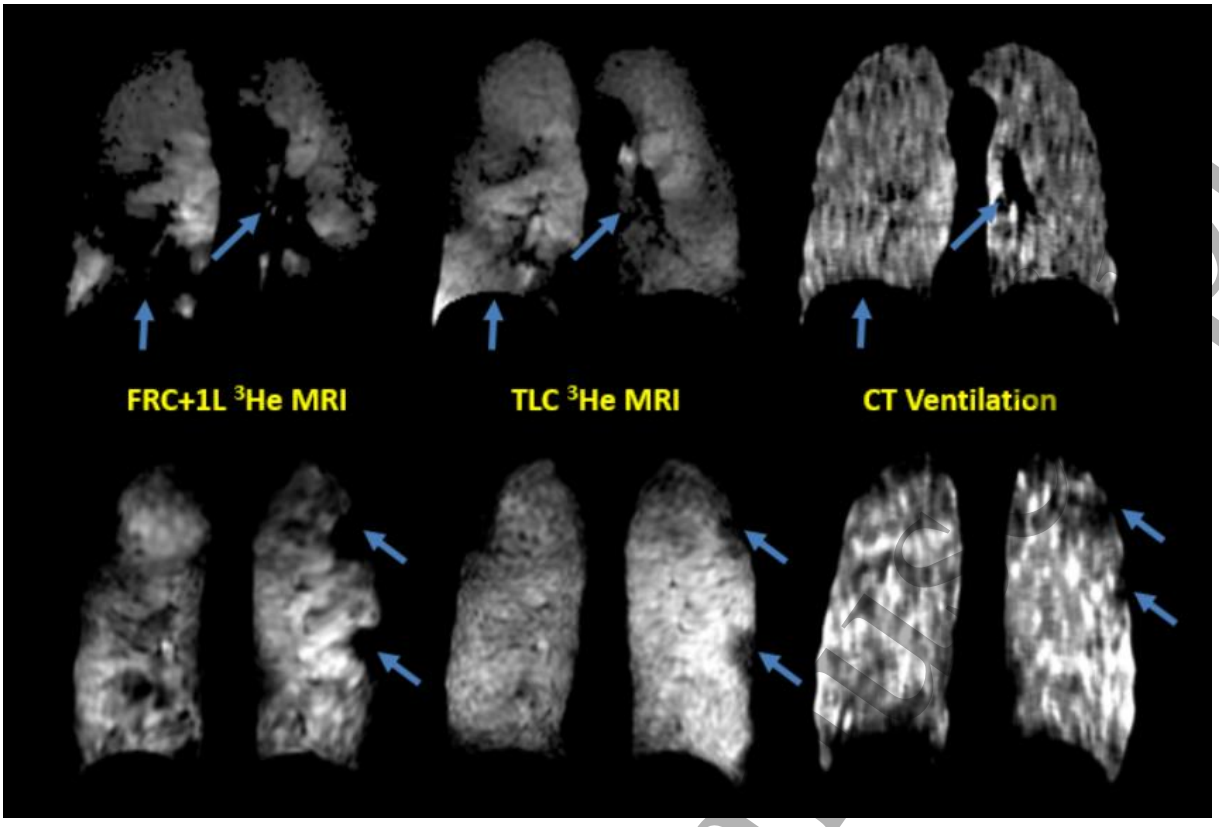

Figure 5 Corresponding coronal slices for two representative patients of registered FRC+1L ^{3}He MRI, TLC ^{3}He MRI and CT ventilation. The blue arrows indicate defects and regions that are more visually similar for CT ventilation and TLC ^{3}He MRI compared with FRC+1L ^{3}He MRI. Note that the lower defect observed in the left lung of the second patient (bottom row) is spatially offset.

Table 3 Dice similarity coefficients for CT ventilation thresholded at two different percentile ranges with FRC+1L and TLC ^{3}He MRI.

	CT 10 to 100% percentile		CT 20 to 100% percentile	
Patients	^{3}He MRI FRC+1L	^{3}He MRI TLC	^{3}He MRI FRC+1L	^{3}He MRI TLC
1	0.86	0.93	0.81	0.87
2	0.78	0.86	0.78	0.84
3	0.92	0.93	0.87	0.88
4	0.92	0.93	0.87	0.87
5	0.68	0.87	0.66	0.83
6	0.92	0.93	0.86	0.87
7	0.85	0.91	0.81	0.86
Mean±SD	0.85±0.09	0.91±0.03	0.81±0.07	0.86±0.02
Median (range)	0.86 (0.68-0.92)	0.93 (0.86-0.93)	0.81 (0.66-0.87)	0.87 (0.83-0.88)
P value	0.017		0.027	

4. Discussion

Seven adults with asthma were evaluated in the first study to compare CT-based surrogates of ventilation with an established ventilation modality acquired at multiple inflation levels. CT ventilation images were more similar to ^{3}He MR ventilation images that were acquired at TLC than at FRC+1L, with significantly higher DSCs between ventilation masks generated from the different modalities when MR images were acquired at TLC. ^{3}He MRI exhibited increased and more homogenous ventilation at TLC than FRC+1L, with several ventilation defects observed at FRC+1L either completely or partially resolved at TLC. The registration of all images to the TLC CT images in this study enabled spatial comparison of ventilation masks generated from the different modalities to examine their similarity on a truly regional basis.

4.1. Breath-hold CT image registration accuracy

The 'EMPIRE10_Syn' pipeline was consistently outperformed by its B-spline analogue. The parameters of both scripts were identical with the exception of regularisation methods for the deformable stage; 'EMPIRE10_Syn' employed Gaussian convolution for regularization whilst 'EMPIRE10_BsplineSyn' employed B-spline functions. These results are in line with that of a previous study in the context of brain registration, where the B-spline Syn algorithm was shown to yield statistically significant improvements in DSCs compared with the well-known Syn algorithm (Tustison and Avants, 2013). Tustison and Avants (2013) have speculated that the improvement could be due to the continuous nature of B-spline regularization when compared to the discrete approximation offered by Gaussian smoothing.

A significant improvement in registration accuracy when compared with the developers' settings was shown for the optimised pipeline developed in this study. Although the developers' settings provided excellent results for the EMPIRE10 challenge data, which comprised of a range of data including 4D-CT and breath-hold, it was not specifically optimised for paired breath-hold CT with extreme motion amplitudes. This demonstrates the importance of problem-specific parameterisation for new registration applications.

4.2. Effect of lung inflation state on distribution of ventilation

Visual evaluation of ventilation-weighted ^{3}He MRI demonstrated increased and more homogenous ventilation at TLC when compared with FRC+1L. In several cases, ventilation defects observed at FRC+1L resolved completely at TLC. This was confirmed by quantitative results where we observed statistically significant improvements in the percent ventilated volumes at the higher inflation state. As lung inflation increases, the increased ventilation homogeneity observed may be attributable to

airway opening and release of trapped air. Brown and Mitzner (1996) used high resolution CT to quantify the effect of lung inflation on airway diameter in canine subjects and observed significant increases at increased inflation levels. Thus, airways that were narrowed or closed at FRC+1L could have opened at the higher inflation state, resolving some of the ventilation defects, as observed in this study.

The results of this study are consistent with other findings suggesting potential bronchodilatory effects of deep inspiration (Scichilone and Togias, 2004). Deep inspirations may enable distribution of gas to hypoventilated regions affected by narrowed or closed airways. Although a degree of ventilation heterogeneity is observed in normal subjects in the form of a vertical gradient due to gravity and other effects, these effects are significantly reduced at TLC where much more homogenous ventilation is observed (Milic-Emili, 2011). Recent work with multi-inflation hyperpolarised gas MRI in healthy subjects and patients with CF has confirmed this hypothesis where increased ventilation heterogeneity was observed at the lower lung volumes with the least ventilation heterogeneity observed at TLC (Hughes *et al.*, 2018; Smith *et al.*, 2018).These results and those observed in the present study suggest that imaging at lower inflation levels is more sensitive at detecting ventilation defects and may be more appropriate to use in routine clinical practice. Notwithstanding, we do believe that there may be a role for multi-inflation hyperpolarised gas MR ventilation imaging by providing information on the nature of reversible airway obstruction in asthma i.e. it may allow discernment of regions of volume-reversible and non-reversible ventilation abnormalities.

Such improvements in ventilation were not observed in this study for all ventilation defects seen, demonstrated by the fact that the percent ventilated volume at TLC was still lower than 100%, despite exhibiting statistically significant improvements from FRC+1L. As such, numerous defects observed at FRC+1L persisted at TLC which we believe to be indicative of less reversible focal airway obstruction. Thus, other factors may have a greater impact on the formation of ventilation defects in asthma including small and large airway closure due to airway inflammation, obstruction and remodelling (Brightling *et al.*, 2012). Importantly, inflammation in the airway smooth muscle bundles has been shown to be a key factor contributing to impaired airway dilation of asthmatics during deep inspiration (Slats *et al.*, 2007).

4.3. Impact of ^{3}He MR inflation level on correlation with CT ventilation

Using DSCs, statistically significant improvements in spatial overlap were observed between CT ventilation and ^{3}He MRI acquired at the higher inflation level of TLC. This might be attributable to the CT acquisition protocol for this study. As the CT-based surrogates were derived from breath-hold

CT acquired at FRC and TLC and thus represent local volume change between these two inflation levels, they would more closely depict the distribution of ^{3}He gas at TLC than at FRC+1L. As mentioned earlier, imaging at FRC+1L appears to be more sensitive at detecting ventilation defects than at TLC and may thus undermine the use of CT ventilation in clinical practice. Whilst we can say that CT ventilation derived from TLC and FRC may not provide measures of ventilation which are as sensitive as FRC+1L ^{3}He MRI at depicting ventilation defects, we cannot say that this will be the case for CT ventilation derived from a different pair of inflation levels. For example, we recently demonstrated that CT ventilation maps derived from FRC and FRC+1L show moderate correlations with hyperpolarised gas MRI and marked ventilation defects (Tahir *et al.*, 2018). To comprehensively answer this question, we require CT acquired at more than two inflation levels (e.g. FRC, FRC+1 and TLC) in order to compare the ventilation distributions of CT ventilation between e.g. FRC & FRC+1L and FRC & TLC to see if there is indeed an increase in ventilation defects with the former. Unfortunately, the acquisition of CT at more than 2 inflation levels was outside the scope of the current imaging protocol but we hope that such a study can be performed in the near future.

Despite notable similarities between CT ventilation and ^{3}He MRI acquired at TLC, perfect correlation was not observed. Visual evaluation demonstrated that some ventilation defects observed on MRI were spatially offset on CT (figure 5). The differences observed between CT and ^{3}He MRI are ultimately attributable to the fact that both modalities provide distinct physiologic measurements; CT-based surrogates of ventilation measure the local change in air volume between two lung inflation states, whilst static ventilation-weighted ^{3}He MR images represent a snapshot of the concentration of ^{3}He gas within the air in the lungs at a given inflation level. As such, the primary purpose of this study was to compare both techniques rather than to validate the CT-based surrogates of ventilation. A more appropriate modality to use for the purpose of validation may be a multiple-breath washout imaging technique such as that described by Horn *et al.* (2014a) which uses ^{3}He MRI as the tracer. By correcting for T1 decay, RF depolarisation and RF coil sensitivity, this technique has the advantage of providing fractional ventilation maps that are fully quantitative. However, this technique is not as widely used and requires more complicated breathing manoeuvers for the patient and much higher doses of hyperpolarised ^{3}He to match the resolution of static ventilation images. This is particular pertinent in the current climax where there is a worldwide paucity of ^{3}He gas. ^{129}Xe is a naturally-abundant isotope for hyperpolarised gas MRI and has demonstrated good correlations with ^{3}He in static lung ventilation and diffusion-weighted MRI (Stewart *et al.*, 2018). We have recently compared both gases with CT ventilation imaging in lung cancer patients and demonstrated moderately low correlations of CT at the voxel-level against both gases, increasing with larger regional analysis, while strong correlations were observed between ^{3}He and ^{129}Xe (Tahir *et al.*, 2018). Technical developments in the field of multiple-breath washout imaging with ^{129}Xe may pave the way for improved comparative studies with CT ventilation imaging.

The findings of this study not only imply the importance of careful volumetric control of lung inflation for CT ventilation validation studies but also for longitudinal studies to monitor disease progression and treatment response. It is, therefore, essential that consistent repeatable breathing manoeuvres are employed as variations can alter the ventilation distributions.

4.4. Study limitations

This study has several limitations. Firstly, a relatively small number of patients were studied; thus, further comprehensive testing on a larger sample size would be beneficial. Nonetheless, we note that the increase in ventilation defects observed at FRC+1L compared with TLC and the increased spatial correlation of CT ventilation imaging with ^{3}He MRI TLC for both percentiles were observed consistently for all subjects studied. Thus, the results are very promising and we believe that it is very likely that these results will be observed for a larger cohort. A larger cohort could also facilitate reliable subgroup analysis, which may aid in understanding the impact of inflation level on the nature and pattern of ventilation defects seen on hyperpolarised gas MR images, across the spectrum of asthma disease, and will allow for a greater understanding of whether the correlations observed between CT and MRI are reproducible across all subgroups.

Furthermore, this study only included patients with asthma. Thus, caution must be exercised when extending these results to other respiratory diseases. For example, although improved airway distention at higher lung inflations has been observed in patients with asthma, albeit to a lower degree than normal subjects (Jensen *et al.*, 2001), comparisons of the effect of deep-inspiration induced changes in airway response between asthma and COPD patients indicate that bronchodilatory effects are less effective in the latter disease (Slats *et al.*, 2007). Therefore, a larger scale study of the effect of inflation level as measured by ^{3}He MRI and its impact on spatial correlation with CT-based ventilation in other respiratory diseases is warranted. Likewise, to further reassure that methods are correlated, it would be useful to perform this study in healthy subjects.

Moreover, CT and MRI were performed several days apart (range: 1 to 4 days); it is well known that asthma symptoms vary over time (Zhang *et al.*, 2002) and thus the degree of airway narrowing and inflammation may have changed between CT and MRI sessions. The present investigation was part of a multi-centre study where patients underwent CT in another city than their MRI scans. Four days was the maximum achievable time for coordinating and organising such a study. Notwithstanding, several patients underwent MRI within a day of CT. To minimise errors associated with reproducibility, we did not recruit patients who had been hospitalized or required high-dose (>10mg prednisolone/day) OCS therapy within 6 weeks of the screening visit. This would have excluded

patients with unstable disease or those who may not have been able to cope with the study procedures, thus ensuring that the patients included in the study were more likely to have stable disease, with less airflow variability over time. We also note that the reproducibility of ^{3}He MRI ventilation distributions in asthma has shown some persistence and reproducibility on the order of a few months (de Lange *et al.*, 2009). However, the authors of this work agree that the comparison of the two imaging modalities might be more appropriately conducted in subjects with relatively fixed ventilation defects such as COPD or stable CF.

Different breath-hold procedures were used for the FRC+1L and TLC ^{3}He MRI acquisitions. For the TLC scans, inhalation of room air would increase the time for the ^{3}He gas to ventilate “slow filling” regions of the lung and may have contributed to the fewer ventilation defects observed at TLC. In previous work with 3D time resolved ^{3}He MRI at breath-hold, we studied the effects of delayed ventilation due to diffusion with time and used this effect to assess co-lateral ventilation pathways due to emphysema (Marshall *et al.*, 2012). In more recent work, we studied the effect of ^{3}He inflation level (TLC and FRC+1L with a similar acquisition protocol to this study) on patients with CF. For that study, we also had collateral ventilation performed for the same patients and demonstrated that no significant changes in ventilation distributions occur within the timescale of 1-3 seconds. However, we appreciate that asthma is a different disease and the effects of delayed ventilation on this timescale are yet to be studied in this patient population and higher homogeneity of ventilation distribution may occur during the additional time for gas to diffuse within 1-3 s. Although this may result in a methodological bias, we believe that this effect is likely to be small.

For determination of ventilated volume, there exists some possibility for erroneous segmentation. For CT ventilation segmentation, numerous techniques have been employed in the literature, most notably, percentile thresholding. Functional percentile ranges used have included 0-20%, 21-40%, 41-60%, 61-80%, 81-100% (Castillo *et al.*, 2010) and 21-100% (Kipritidis *et al.*, 2014). Here, we employed two percentile ranges and observed that the 10-100th functional percentile range exhibited greater correlation with the ^{3}He MRI segmentation than that of the 20-100th range, suggesting that spatial correlation between modalities is sensitive to CT ventilation segmentation technique. Similarly, with the relative infancy of hyperpolarised gas MRI as a tool to assess pulmonary ventilation distribution, no definitive consensus yet exists regarding best practice on segmentation and delineation of ventilated volume. In particular, similar to Kirby *et al.* (2012), we classified regions of hypointense signal as part of ventilated volume. This will inevitably lead to reduced defect volumes when compared to other groups who classify hypointense signal as a defect.

DSCs provide a measure of overlap between two binary segmentations and do not account for subtler differences in the intensity distributions within the boundaries of these segmentations. A more

robust method of comparing the images would be to perform voxel-wise spatial correlations as has been performed for Galligas PET and CT ventilation images which were acquired on the same scanner and were thus inherently co-registered (Kipritidis *et al.*, 2014). However, in this study, no strict patient immobilization protocol was observed when acquiring ^{3}He MRI and CT, leading to significant postural differences and images were acquired several days apart. Furthermore, ^{3}He MRI resolution was significantly lower than that of CT, especially in the z direction (10mm vs. 1mm). The CT and MRI registration accuracy, computed via TRE, has previously been assessed for this cohort to be on order of > 10 mm (Tahir *et al.*, 2014). As such, these significant differences in acquisition settings between CT and MRI precluded us from performing a meaningful voxel-wise correlation. An improved acquisition strategy such as that proposed by Ireland *et al.* (2008) where MRI and CT are acquired on the same day with matching subject immobilisation palettes may mitigate these limitations. Moreover, recent advancements in MR image acquisition have led to improved resolution and image quality of same-breath ^{3}He and ^{1}H MRI (Horn *et al.*, 2014b).

For ^{3}He MRI, patients inhaled the noble gas from a starting point of FRC until they reached the desired inflation level. Inhalation from residual volume has been shown to provide different gas distributions (Milic-Emili *et al.*, 1966) and may result in different correlations. Similarly, CT breathing manoeuvre has been shown to alter the resulting ventilation distribution (Mistry *et al.*, 2013). In this study, we did not acquire CT at FRC+1L. Given our findings, we hypothesise that CT acquired at FRC and FRC+1L would lead to ventilation surrogates more closely matched to ^{3}He MRI acquired at FRC+1L, compared with ventilation computed from CT acquired at FRC and TLC.

5. Conclusion

This study demonstrates that comparison of CT ventilation and hyperpolarised gas MRI varies with inflation state during gas MRI. If CT is acquired at FRC and TLC, a higher correlation with gas ventilation MR imaging can be achieved if the latter is acquired at TLC. This study also provides further evidence that ventilation abnormalities are sensitive to inflation level and that imaging at lower lung volumes may be more sensitive at depicting ventilation defects. Imaging at multiple inflation levels may facilitate discernment of regions of volume-reversible and non-reversible ventilation defects. Further work is needed to determine the optimal inflation levels for CT ventilation imaging.

Acknowledgements

This work was supported by the University of Sheffield James Morrison Fund, Sheffield Hospitals Charity, Weston Park Hospital Cancer Charity, National Institute of Health Research, AirPROM (EU FP7) and Novartis.

References

Avants B B, Epstein C L, Grossman M and Gee J C 2008 Symmetric diffeomorphic image registration with cross-correlation: evaluating automated labeling of elderly and neurodegenerative brain *Med Image Anal* **12** 26-41

Avants B B, Tustison N J, Song G, Cook P A, Klein A and Gee J C 2011 A reproducible evaluation of ANTs similarity metric performance in brain image registration *Neuroimage* **54** 2033-44

Brightling C E, Gupta S, Gonem S and Siddiqui S 2012 Lung damage and airway remodelling in severe asthma *Clin Exp Allergy* **42** 638-49

Brown R H and Mitzner W 1996 Effect of lung inflation and airway muscle tone on airway diameter in vivo *J Appl Physiol (1985)* **80** 1581-8

Castillo R, Castillo E, Fuentes D, Ahmad M, Wood A M, Ludwig M S and Guerrero T 2013 A reference dataset for deformable image registration spatial accuracy evaluation using the COPDgene study archive *Phys Med Biol* **58** 2861-77

Castillo R, Castillo E, Martinez J and Guerrero T 2010 Ventilation from four-dimensional computed tomography: density versus Jacobian methods *Phys Med Biol* **55** 4661-85

Castillo R, Castillo E, McCurdy M, Gomez D R, Block A M, Bergsma D, Joy S and Guerrero T 2012 Spatial correspondence of 4D CT ventilation and SPECT pulmonary perfusion defects in patients with malignant airway stenosis *Phys Med Biol* **57** 1855-71

Christian J A, Partridge M, Nioutsikou E, Cook G, McNair H A, Cronin B, Courbon F, Bedford J L and Brada M 2005 The incorporation of SPECT functional lung imaging into inverse radiotherapy planning for non-small cell lung cancer *Radiother Oncol* **77** 271-7

Chuang K-S, Tzeng H-L, Chen S, Wu J and Chen T-J 2006 Fuzzy c-means clustering with spatial information for image segmentation *Computerized Medical Imaging and Graphics* **30** 9-15

Crawford A B, Makowska M, Paiva M and Engel L A 1985 Convection- and diffusion-dependent ventilation maldistribution in normal subjects *J Appl Physiol (1985)* **59** 838-46

de Lange E E, Altes T A, Patrie J T, Battiston J J, Juersivich A P, Mugler J P, 3rd and Platts-Mills T A 2009 Changes in regional airflow obstruction over time in the lungs of patients with asthma: evaluation with 3He MR imaging *Radiology* **250** 567-75

Glocker B, Sotiras A, Komodakis N and Paragios N 2011 Deformable Medical Image Registration: Setting the State of the Art with Discrete Methods *Annu Rev Biomed Eng* **13** 219-44

Guerrero T, Sanders K, Noyola-Martinez J, Castillo E, Zhang Y, Tapia R, Guerra R, Borghero Y and Komaki R 2005 Quantification of regional ventilation from treatment planning CT *Int J Radiat Oncol Biol Phys* **62** 630-4

Horn F C, Deppe M H, Marshall H, Parra-Robles J and Wild J M 2014a Quantification of regional fractional ventilation in human subjects by measurement of hyperpolarized 3He washout with 2D and 3D MRI *J Appl Physiol (1985)* **116** 129-39

Horn F C, Tahir B A, Stewart N J, Collier G J, Norquay G, Leung G, Ireland R H, Parra-Robles J, Marshall H and Wild J M 2014b Lung ventilation volumetry with same-breath acquisition of hyperpolarized gas and proton MRI *NMR Biomed* **27** 1461-7

Hughes P J C, Horn F C, Collier G J, Biancardi A, Marshall H and Wild J M 2017 Spatial fuzzy c-means thresholding for semiautomated calculation of percentage lung ventilated volume from hyperpolarized gas and (1) H MRI *J Magn Reson Imaging*

Hughes P J C, Smith L, Chan H F, Tahir B A, Norquay G, Collier G J, Biancardi A M, Marshall H and Wild J M 2018 Assessment of the influence of lung inflation state on the

quantitative parameters derived from hyperpolarized gas lung ventilation MRI in healthy volunteers *J Appl Physiol (1985)*

Ireland R H, Bragg C M, McJury M, Woodhouse N, Fichele S, van Beek E J, Wild J M and Hatton M Q 2007 Feasibility of image registration and intensity-modulated radiotherapy planning with hyperpolarized helium-3 magnetic resonance imaging for non-small-cell lung cancer *Int J Radiat Oncol Biol Phys* **68** 273-81

Ireland R H, Tahir B A, Wild J M, Lee C E and Hatton M Q 2016 Functional Image-guided Radiotherapy Planning for Normal Lung Avoidance *Clin Oncol (R Coll Radiol)* **28** 695-707

Ireland R H, Woodhouse N, Hoggard N, Swinscoe J A, Foran B H, Hatton M Q and Wild J M 2008 An image acquisition and registration strategy for the fusion of hyperpolarized helium-3 MRI and x-ray CT images of the lung *Phys Med Biol* **53** 6055-63

Jensen A, Atileh H, Suki B, Ingenito E P and Lutchen K R 2001 Selected contribution: airway caliber in healthy and asthmatic subjects: effects of bronchial challenge and deep inspirations *J Appl Physiol (1985)* **91** 506-15; discussion 4-5

Kipritidis J, Siva S, Hofman M S, Callahan J, Hicks R J and Keall P J 2014 Validating and improving CT ventilation imaging by correlating with ventilation 4D-PET/CT using 68Ga-labeled nanoparticles *Med Phys* **41** 011910

Kirby M, Heydarian M, Svenningsen S, Wheatley A, McCormack D G, Etemad-Rezai R and Parraga G 2012 Hyperpolarized 3He magnetic resonance functional imaging semiautomated segmentation *Acad Radiol* **19** 141-52

Kurose T, Okumura Y, Sato S, Yamamoto Y, Akaki S, Takeda Y, Kanazawa S, Ando A, Date H, Shimizu N and Hiraki Y 2004 Functional evaluation of lung by Xe-133 lung ventilation scintigraphy before and after lung volume reduction surgery (LVRS) in patients with pulmonary emphysema *Acta Med Okayama* **58** 7-15

Latifi K, Forster K M, Hoffe S E, Dilling T J, van Elmpt W, Dekker A and Zhang G G 2013 Dependence of ventilation image derived from 4D CT on deformable image registration and ventilation algorithms *J Appl Clin Med Phys* **14** 4247

Marshall H, Deppe M H, Parra-Robles J, Hillis S, Billings C G, Rajaram S, Swift A, Miller S R, Watson J H, Wolber J, Lipson D A, Lawson R and Wild J M 2012 Direct visualisation of collateral ventilation in COPD with hyperpolarised gas MRI *Thorax* **67** 613-7

Marshall H, Siddiqui S, Leung G, Parra-Robles J, Xu X, Brightling C and Wild J 2013 Imaging The Effect Of Airway Opening In Asthma Due To Inflation State With 3He MRI *Am J Respir Crit Care Med* **187** A3744

Mathew L, Wheatley A, Castillo R, Castillo E, Rodrigues G, Guerrero T and Parraga G 2012 Hyperpolarized (3)He magnetic resonance imaging: comparison with four-dimensional x-ray computed tomography imaging in lung cancer *Acad Radiol* **19** 1546-53

Milic-Emili J 2011 *Comprehensive Physiology*: John Wiley & Sons, Inc.)

Milic-Emili J, Henderson J A, Dolovich M B, Trop D and Kaneko K 1966 Regional distribution of inspired gas in the lung *J Appl Physiol* **21** 749-59

Mistry N N, Diwanji T, Shi X, Pokharel S, Feigenberg S, Scharf S M and D'Souza W D 2013 Evaluation of fractional regional ventilation using 4D-CT and effects of breathing maneuvers on ventilation *Int J Radiat Oncol Biol Phys* **87** 825-31

Mugler J P, 3rd, Altes T A, Ruset I C, Dregely I M, Mata J F, Miller G W, Ketel S, Ketel J, Hersman F W and Ruppert K 2010 Simultaneous magnetic resonance imaging of ventilation distribution and gas uptake in the human lung using hyperpolarized xenon-129 *Proc Natl Acad Sci U S A* **107** 21707-12

Muradyan I, Loring S H, Ferrigno M, Lindholm P, Topulos G P, Patz S and Butler J P 2010 Inhalation heterogeneity from subresidual volumes in elite divers *J Appl Physiol (1985)* **109** 1969-73

Murphy K, van Ginneken B, Reinhardt J M, Kabus S, Ding K, Deng X, Cao K, Du K, Christensen G E, Garcia V, Vercauteren T, Ayache N, Commowick O, Malandain G, Glocker B, Paragios N, Navab N, Gorbunova V, Sporring J, de Bruijne M, Han X, Heinrich M P, Schnabel J A, Jenkinson M, Lorenz C, Modat M, McClelland J R, Ourselin S, Muenzing S E, Viergever M A, De Nigris D, Collins D L, Arbel T, Peroni M, Li R, Sharp G C, Schmidt-Richberg A, Ehrhardt J, Werner R, Smeets D, Loeckx D, Song G, Tustison N, Avants B, Gee J C, Staring M, Klein S, Stoel B C, Urschler M, Werlberger M, Vandemeulebroucke J, Rit S, Sarrut D and Pluim J P 2011 Evaluation of registration methods on thoracic CT: the EMPIRE10 challenge *IEEE Trans Med Imaging* **30** 1901-20

Reinhardt J M, Ding K, Cao K, Christensen G E, Hoffman E A and Bodas S V 2008 Registration-based estimates of local lung tissue expansion compared to xenon CT measures of specific ventilation *Med Image Anal* **12** 752-63

Scichilone N and Togias A 2004 The role of lung inflation in airway hyperresponsiveness and in asthma *Curr Allergy Asthma Rep* **4** 166-74

Seppenwoolde Y, Engelsman M, De Jaeger K, Muller S, Belderbos J, Boersma L and Lebesque J 2000 Optimising radiation treatment plans for lung cancer using functional information *Radiotherapy and Oncology* **56**

Slats A M, Janssen K, van Schadewijk A, van der Plas D T, Schot R, van den Aardweg J G, de Jongste J C, Hiemstra P S, Mauad T, Rabe K F and Sterk P J 2007 Bronchial inflammation and airway responses to deep inspiration in asthma and chronic obstructive pulmonary disease *Am J Respir Crit Care Med* **176** 121-8

Smith L J, Collier G J, Marshall H, Hughes P J C, Biancardi A M, Wildman M, Aldag I, West N, Horsley A and Wild J M 2018 Patterns of regional lung physiology in cystic fibrosis using ventilation magnetic resonance imaging and multiple-breath washout *Eur Respir J* **52**

Stewart N J, Chan H F, Hughes P J C, Horn F C, Norquay G, Rao M, Yates D P, Ireland R H, Hatton M Q, Tahir B A, Ford P, Swift A J, Lawson R, Marshall H, Collier G J and Wild J M 2018 Comparison of (3) He and (129) Xe MRI for evaluation of lung microstructure and ventilation at 1.5T *J Magn Reson Imaging* **0**

Tahir B A, Hughes P J C, Robinson S D, Marshall H, Stewart N J, Norquay G, Biancardi A, Chan H F, Collier G J, Hart K A, Swinscoe J A, Hatton M Q, Wild J M and Ireland R H 2018 Spatial comparison of CT-based surrogates of lung ventilation with hyperpolarized Helium-3 and Xenon-129 gas MRI in patients undergoing radiation therapy *International Journal of Radiation Oncology*Biology*Physics*

Tahir Bilal A, Swift Andrew J, Marshall H, Parra-Robles J, Hatton Matthew Q, Hartley R, Kay R, Brightling Christopher E, Vos W, Wild Jim M and Ireland Rob H 2014 A method for quantitative analysis of regional lung ventilation using deformable image registration of CT and hybrid hyperpolarized gas/ 1 H MRI *Phys Med Biol* **59** 7267

Tahir B A, Van Holsbeke C, Ireland R H, Swift A J, Horn F C, Marshall H, Kenworthy J C, Parra-Robles J, Hartley R, Kay R, Brightling C E, De Backer J, Vos W and Wild J M 2016 Comparison of CT-based Lobar Ventilation with 3He MR Imaging Ventilation Measurements *Radiology* **278** 585-92

Thomen R P, Sheshadri A, Quirk J D, Kozlowski J, Ellison H D, Szczesniak R D, Castro M and Woods J C 2015 Regional ventilation changes in severe asthma after bronchial thermoplasty with (3)He MR imaging and CT *Radiology* **274** 250-9

Tomasi C and Manduchi R 1998 Bilateral Filtering for Gray and Color Images. In: *Proceedings of the Sixth International Conference on Computer Vision*: IEEE Computer Society) p 839

Tustison N J and Avants B B 2013 Explicit B-spline regularization in diffeomorphic image registration *Front Neuroinform* **7** 39

Vandemeulebroucke J, Rit S, Kybic J, Clarysse P and Sarrut D 2011 Spatiotemporal motion estimation for respiratory-correlated imaging of the lungs *Med Phys* **38** 166-78

Wild J M, Ajraoui S, Deppe M H, Parnell S R, Marshall H, Parra-Robles J and Ireland R H 2011 Synchronous acquisition of hyperpolarised 3He and 1H MR images of the lungs - maximising mutual anatomical and functional information *NMR Biomed* **24** 130-4

Yamamoto T, Kabus S, Klinder T, von Berg J, Lorenz C, Loo B W, Jr. and Keall P J 2011 Four-dimensional computed tomography pulmonary ventilation images vary with deformable image registration algorithms and metrics *Med Phys* **38** 1348-58

Yamamoto T, Kabus S, Lorenz C, Mittra E, Hong J C, Chung M, Eclov N, To J, Diehn M, Loo B W, Jr. and Keall P J 2014 Pulmonary ventilation imaging based on 4-dimensional computed tomography: comparison with pulmonary function tests and SPECT ventilation images *Int J Radiat Oncol Biol Phys* **90** 414-22

Zhang J, Yu C, Holgate S T and Reiss T F 2002 Variability and lack of predictive ability of asthma end-points in clinical trials *Eur Respir J* **20** 1102-9